# Mechanistic Proposals for Direct Benzene Hydroxylation over Fe−ZSM-5 Zeolite

**Kazunari Yoshizawa,* Yoshihito Shiota, and Takashi Kamachi**

*Institute for Materials Chemistry and Engineering, Kyushu University, Fukuoka 812-8581, Japan*

*Received: February 25, 2003; In Final Form: June 20, 2003*

A mechanism of direct benzene hydroxylation over Fe−ZSM-5 zeolite is discussed from B3LYP density functional theory computations. We demonstrate using a mononuclear iron model supported at the $AlO_4^-$ site of zeolite that Fe−ZSM-5 zeolite reasonably catalyzes the conversion of benzene to phenol with $N_2O$. A key in this catalytic reaction is that benzene hydroxylation and $N_2O$ decomposition occur at the same active site in a well-balanced manner. In the initial stages of the reaction, a reactive oxygen species referred to as "α-oxygen" is formed upon decomposition of $N_2O$ at the iron active site. The first reaction step is the formation of a complex between benzene and the α-oxygen species. The C−H activation of benzene leads to an intermediate that involves OH and $C_6H_5$ groups as ligands. After forming this intermediate, the reaction has a junction that leads to two possible pathways, depending on the concentration of $N_2O$. The recombination between the OH and $C_6H_5$ ligands, which leads to a complex of phenol, can occur when the concentration of $N_2O$ is low, whereas the decomposition of nitrous oxide can occur on the intermediate involving OH and $C_6H_5$ groups when the $N_2O$ concentration is sufficiently high. Calculated potential energy diagrams and reaction kinetics show that the latter pathway is energetically more favorable than the former. We propose that benzene hydroxylation over Fe−ZSM-5 zeolite should proceed in the following way: (1) the formation of the benzene complex at the iron active site, (2) the hydrogen abstraction from benzene, (3) the decomposition of $N_2O$ at the active site, (4) the recombination between the OH and $C_6H_5$ ligands, and (5) the release of product phenol.

## Introduction

Benzene is directly converted into phenol with nitrous oxide ($N_2O$) as an oxidizing reagent over transition-metal oxides supported on silica gel[1] and over ZSM-5 zeolite.[2,3] This one-step conversion indicated in reaction 1 is thermodynamically

$$N_2O + C_6H_6 \rightarrow N_2 + C_6H_5OH \quad (1)$$

efficient compared to the commercial two-step process via cumen.[4] Panov and collaborators[2] have suggested that the high reactivity of ZSM-5 zeolite should be ascribed to impurity iron, which is added mainly along with the starting ingredients at the step of zeolite synthesis. The selectivity for phenol using samples of ZSM-5 containing 0.07−0.72 wt % of iron calculated for $Fe_2O_3$ is 100% at 20−25% conversion levels of benzene at 300−400 °C. A surface oxygen species generated over Fe−ZSM-5 zeolite under the decomposition of nitrous oxide, as indicated by (O) in reaction 2a, has been proposed to be responsible for the formation of phenol from benzene (reaction 2b). Such an oxygen species is called "α-oxygen".[2] Although

$$N_2O + (X) \rightarrow (O) + N_2 \quad (2a)$$

$$(O) + C_6H_6 \rightarrow (X) + C_6H_5OH \quad (2b)$$

this active species has not yet been characterized in detail, it is probably a kind of iron-oxo species. Methane also reacts with "α-oxygen" to give methanol as a product,[5] but the hydroxylation of methane is limited to a single turnover reaction.

Despite lots of attempts to detect and characterize "α-oxygen", there is no detailed structural information on this active species.[6] Mössbauer and EXAFS analyses of Fe−ZSM-5 zeolite suggested that "α-oxygen" should involve high-spin Fe(III) and Fe(II) ions.[5b,7−10] Shilov and Steinman[10] suggested that methane hydroxylation over Fe−ZSM-5 is a good functional model in considering the mechanism of soluble methane monooxygenase (sMMO).[11] Zhidomirov and co-workers[12] discussed the decomposition of nitrous oxide using both mononuclear and dinuclear iron complexes as active site models of "α-oxygen" from MP2 and density functional theory (DFT) calculations and concluded that the dinuclear complex is catalytically more active. Joyner and Stockenhuber[13] indicated that there are two different iron−oxo candidates on the surface of ZSM-5 zeolite, i.e., a mononuclear iron species and an iron nanocluster. Thus, two possible structures are available at present with respect to "α-oxygen"; one possibility is an isolated iron−oxo species and the other is an oxygen-bridged dinuclear iron species. Feng and Hall proposed that the formation of the oxygen-bridged diiron structure is limited in Fe−ZSM-5 when the Si/Al ratio ($x$) falls within a commonly employed region $11 < x < 25$.[14] Moreover, Bell et al. demonstrated from DFT calculations on the decomposition of nitrous oxide that isolated metal−oxo cations such as $[FeO]^+$ and $[CoO]^+$ can serve as active centers of ZSM-5 zeolite.[15]

In previous papers[16] we assumed a monoiron species to be supported on the $AlO_4^-$ site of ZSM-5 zeolite (the so-called Brønsted acid site), as shown in Scheme 1, and discussed the formation of "α-oxygen" using this active site model and hydroxylation reactions at this active site. Although this is a minimal model that mimics the coordination sphere of the $AlO_4^-$ site, it is useful in considering essential aspects of hydroxylation reactions over Fe−ZSM-5. We considered that the benzene and

* To whom correspondence should be addressed. E-mail: kazunari@ms.ifoc.kyushu-u.ac.jp.

10.1021/jp030240b CCC: $25.00 
Published on Web 09/23/2003

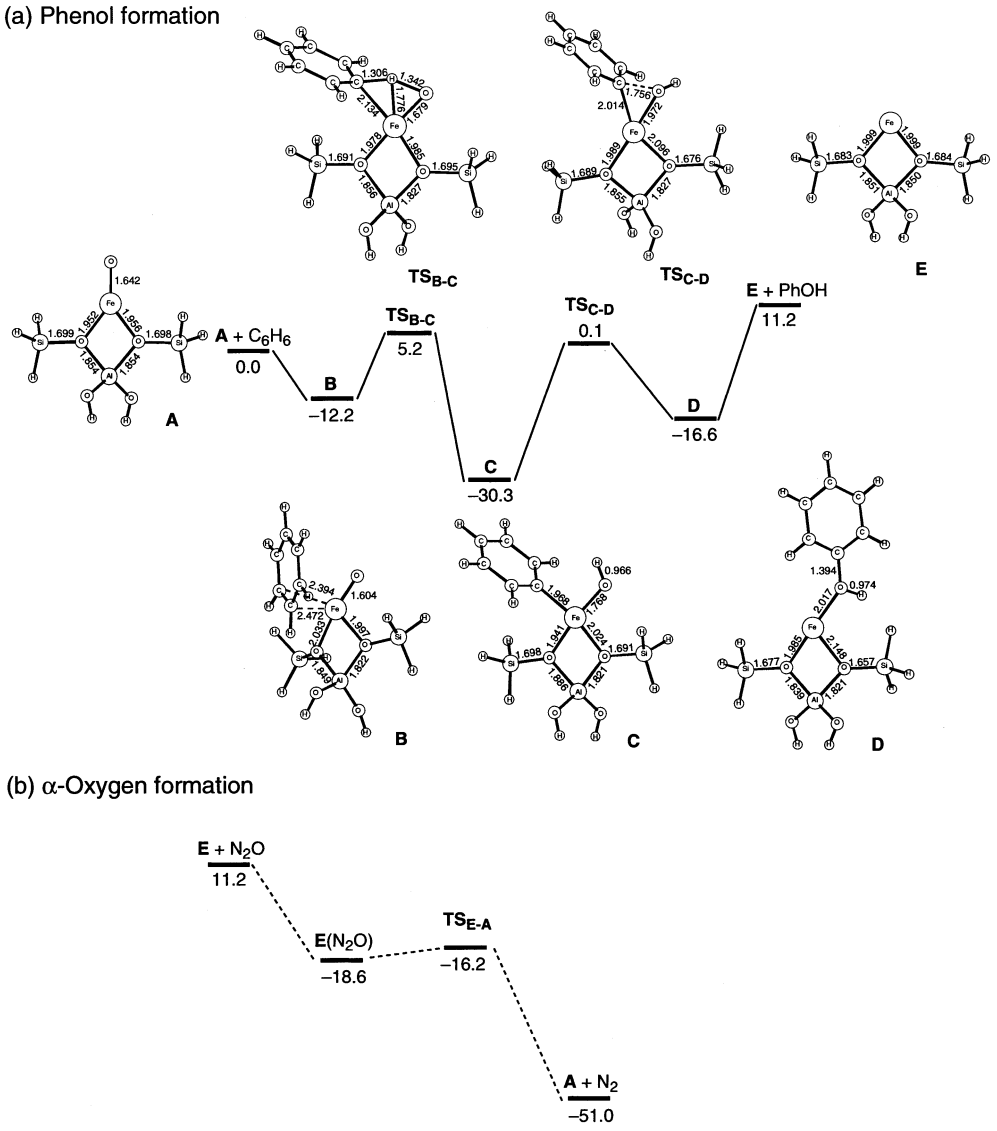


**Figure 1.** Potential energy diagrams in the quartet state for (a) the direct benzene hydroxylation and (b) the formation of "α-oxygen". Relative energies are in kcal/mol. Dotted lines indicate a potential energy diagram in the sextet state.[16a]

**SCHEME 1**

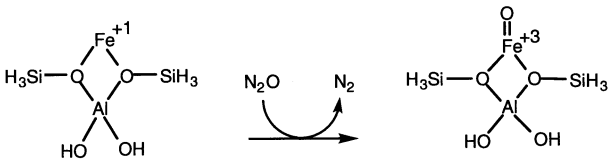


methane hydroxylation reactions over Fe−ZSM-5 have important relevance to those of various hydroxylation reactions by the bare $FeO^+$ complex in that this active species is generated by the reaction between $Fe^+$ and nitrous oxide in a similar manner in the gas phase.[17] Schwarz and collaborators have carried out detailed analyses of various gas-phase reactions of $FeO^+$ with methane, higher alkanes, alkenes, benzene, and other [C,H,O] compounds.[18] The $FeO^+$ complex converts benzene to phenol in 56% yield.[19] In this reaction nitrous oxide is also used as an oxidizing reagent. We have investigated from DFT calculations how the bare $FeO^+$ complex activates the C−H bonds of methane,[20] benzene,[21] and related compounds.[22]

Thus, the diverse reactivity of $FeO^+$ is of great use in considering the reaction mechanism of Fe−ZSM-5 that should involve an iron−oxo species at the active center. DFT calculations demonstrated that the mononuclear model indicated in Scheme 1 can mediate the direct reactions of benzene to phenol and of methane to methanol;[16b] however, the computed energetics is unfavorable in the exit channel because an Fe(I) species is inevitably formed in the proposed mechanism. The presence of an Fe(I) species is not in agreement with the Mössbauer measurements of Fe−ZSM-5 zeolite as well as a general trend that Fe(I) species are rare in solids. One of the reviewers of our paper[16b] suggested that a dinuclear iron active site like in sMMO allows more reasonable reduction of the Fe(III)/Fe(III) state to the Fe(II)/Fe(II) state in the catalytic cycle although intermediate Q of sMMO that catalyzes methane hydroxylation under physiological conditions is widely believed to involve an Fe(IV)Fe(IV) species.[11] To address this comment, we propose on the basis of the same monoiron model a new catalytic mechanism in which no Fe(I) species is involved.

## Method of Calculation

We optimized local minima and saddle points on potential energy surfaces using the B3LYP hybrid DFT method,[23,24] which has been reported to provide excellent descriptions of various reaction profiles, particularly in geometries, heats of reaction, barrier heights, and vibrational frequencies.[25] For the Fe atom we used the (16s10p6d) primitive set of Wachters[26]

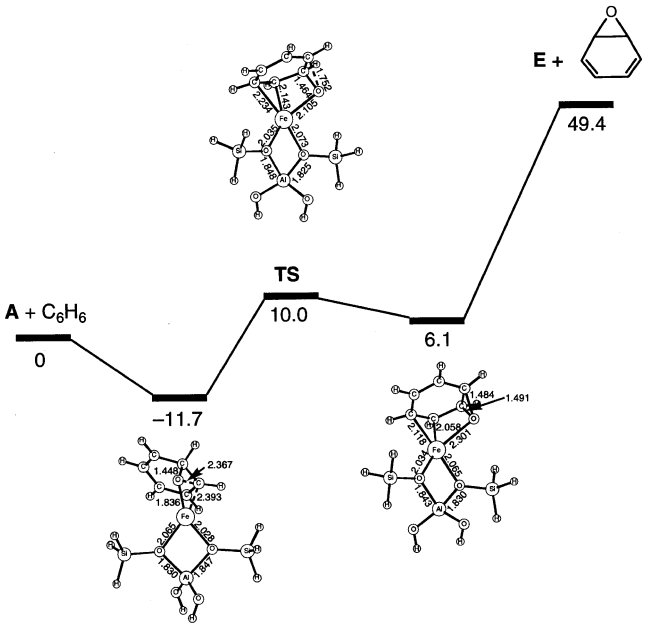


**Figure 2.** Potential energy diagram for the arene−epoxide pathway in the quartet state.

and Hay[27] supplemented with one polarization f-function ($\alpha$ = 1.05 for Fe),[28] and for the H, C, O, Al, and Si atoms we used the D95** basis set,[29] a standard double-$\zeta$ basis set with polarization functions. Systematic vibrational analyses characterized stable structures to have no imaginary mode of vibration and transition states to have only one imaginary mode. We used the Gaussian 98 program package[30] for these DFT calculations.

## Results and Discussion

**Overview of the Previous Mechanism.** Let us first look at a reaction pathway for benzene hydroxylation over Fe−ZSM-5. Because we described the results in detail in the previous paper,[16b] here we refer to essential aspects on the reaction pathway. The potential energy surface of the spin quartet state plays a major role in this reaction like in benzene hydroxylation by $FeO^+$,[21] in contrast to methane hydroxylation in which both quartet and sextet surfaces play an important role. Optimized structures of the reaction species are shown in Figure 1. The first step of the reaction is the formation of the benzene complex B that involves benzene as a ligand in an $\eta^2$-coordination manner. The bound benzene molecule undergoes a hydrogen abstraction via the transition state $TS_{B-C}$ to form intermediate C. This intermediate involves a four-coordinate iron atom that has hydroxo and phenyl ligands. In the next step the rebound reaction between the hydroxo and phenyl ligands takes place at the iron active center via the transition state $TS_{C-D}$, leading to intermediate D. This catalytic reaction is completed by the release of product phenol. The mechanism proposed here involves H-atom abstraction as an essential process in the initial stages of the reaction. However, this is not in agreement with the mechanism via arene−epoxide formation that Panov and collaborators have proposed from isotope labeling experiments.[2g] To look at which mechanism is energetically more feasible, we carried out DFT calculations about the oxo insertion to a C−C bond of the benzene ring. The oxo-insertion pathway that leads to the formation of arene−epoxide was calculated to lie in energy above that for the H-atom abstraction pathway, due to the deformation of the resonance structure of the benzene ring in the oxo-insertion mechanism; see Figure 2. In view of this computational result, it is reasonable to consider that benzene hydroxylation over Fe−ZSM-5 zeolite should proceed via the H-atom abstraction rather than the epoxide formation.

Figure 1a shows a computed potential energy diagram along the direct benzene hydroxylation pathway over Fe−ZSM-5 in the quartet state, $C_6H_6 + N_2O \rightarrow C_6H_5OH + N_2$, in which the energy is relative to the dissociation limit of A + benzene. The benzene complex B lies 12.2 kcal/mol below the dissociation limit, which shows that the benzene molecule is strongly bound to the active site. The activation energy for the hydrogen abstraction via $TS_{B-C}$ is 17.4 kcal/mol relative to B, whereas an energy of 5.2 kcal/mol is necessary to pass over $TS_{B-C}$ if we assume that the reaction proceeds under adiabatic conditions. This small activation barrier for $TS_{B-C}$ is fully consistent with an experimental result that benzene is converted to phenol over Fe−ZSM-5 zeolite at low temperature.[5]

The next step of the reaction pathway is the formation of intermediate D via $TS_{C-D}$ that corresponds to the rebound reaction between the hydroxo and phenyl ligands of intermediate C. The relative energies of $TS_{C-D}$ and D were calculated to be +0.1 and −16.6 kcal/mol, respectively. However, the release of phenol from D requires an activation energy of 27.8 kcal/mol relative to D, and intermediate E is 11.2 kcal/mol less stable than the dissociation limit. Thus, the overall reaction is endothermic, and intermediate E is energetically less stable than the two important transition states $TS_{B-C}$ and $TS_{C-D}$. This energetical instability is clearly due to the formation of the Fe(I) center in the mechanism for the catalytic function of Fe−ZSM-5 zeolite.

We investigated the decomposition of nitrous oxide at the Fe(I) center of the $AlO_4^-$ site of zeolite.[16a] The binding energy between intermediate E and nitrous oxide is 29.8 kcal/mol, and the decomposition of nitrous oxide requires only 2.4 kcal/mol, as shown in Figure 1b. Thus, nitrous oxide is strongly bound to the active iron site and easily decomposes into dinitrogen and "$\alpha$-oxygen"; this process is exothermic by nearly 60 kcal/mol on the sextet potential energy surface. The calculated energetics suggested that "$\alpha$-oxygen" regenerated upon decomposition of nitrous oxide can repeat the benzene-to-phenol conversion if the release of phenol occurs to form the unstable intermediate E. However, because the reaction toward E is energetically unfavorable, we should find a reaction pathway that does not involve such an unstable Fe(I) species for a better catalytic mechanism.

**Role of $N_2O$ Decomposition in the Catalysis.** The decomposition of nitrous oxide can play a key role in starting a new catalytic cycle of benzene hydroxylation. To improve the mechanism discussed above, we considered how the decomposition of nitrous oxide occurs in the course of the reaction. One can expect that the insertion of an oxygen atom should take place upon decomposition of nitrous oxide on a stable intermediate. The general profile of the energy diagram in Figure 1a suggests that the oxygen insertion is likely to occur on intermediate C or D. Resultant intermediates referred to as F and G can be formed according to reactions 3 and 4, respectively.

$$N_2O + C \rightarrow TS_{C-F} \rightarrow N_2 + F \quad (3)$$

$$N_2O + D \rightarrow TS_{D-G} \rightarrow N_2 + G \quad (4)$$

where $TS_{C-F}$ ($TS_{D-G}$) is a transition state in which the N−O bond cleavage and the Fe−O bond formation occur in a concerted manner to connect intermediates C and F (D and G). These pathways can, of course, proceed without the formation of the unfavorable Fe(I) state through the formation of the Fe-

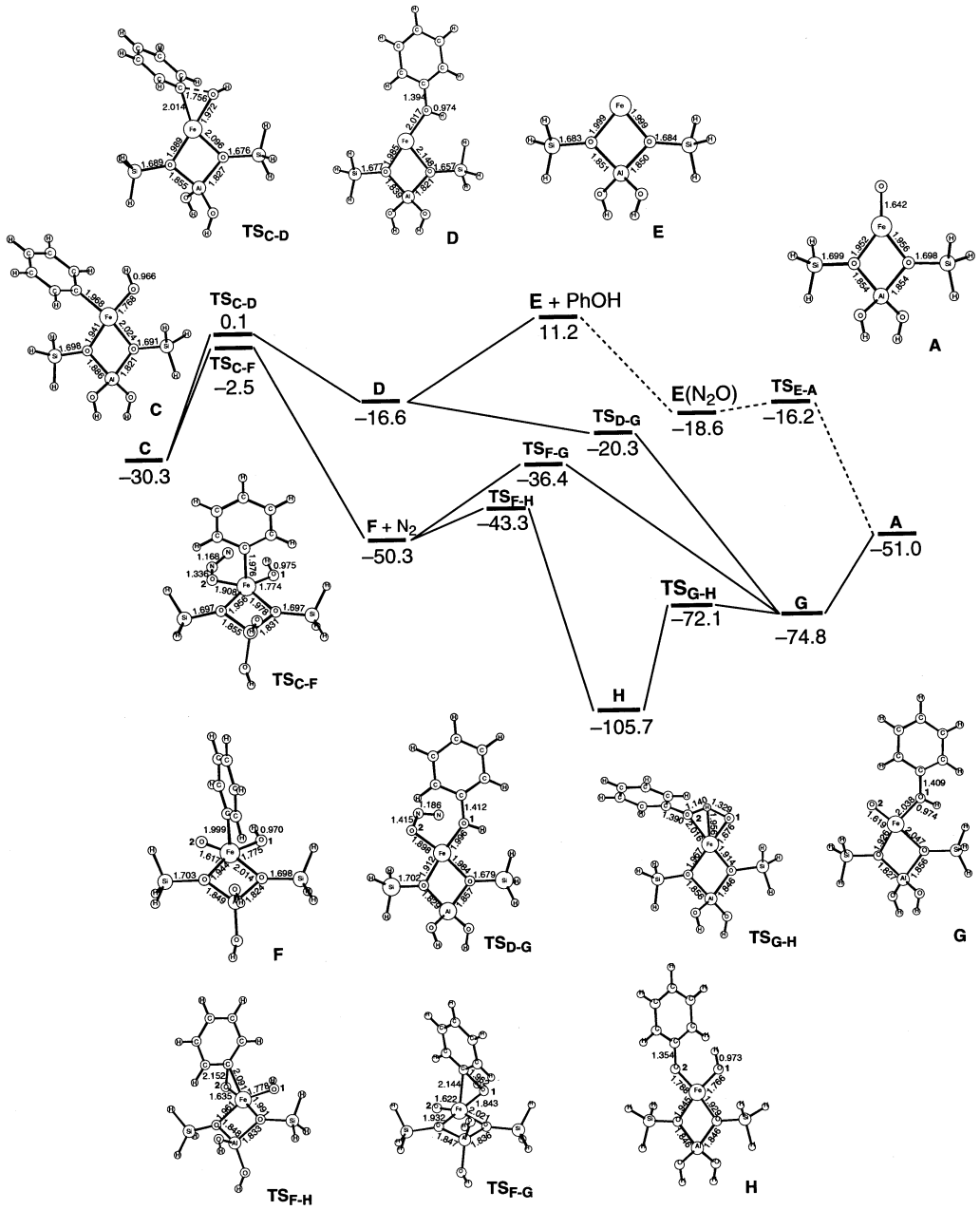


**Figure 3.** Energy diagrams and reaction species for the pathways from intermediate C to the formation of phenol and "α-oxygen" of Fe−ZSM-5 zeolite. The energies are relative to the dissociation limit of A + benzene in units of kcal/mol. Dotted lines indicate the sextet potential energy diagram.

(V) species on intermediate F and the Fe(III) species on intermediate G. Optimized structures of $TS_{C-F}$, F, $TS_{D-G}$, and G are presented in Figure 3. The $N-O^2$ and $Fe-O^2$ distances of $TS_{C-F}$ ($TS_{D-G}$) are 1.336 (1.415) and 1.908 (1.898) Å, respectively. The $N-O^2$ distance of $TS_{C-F}$ ($TS_{D-G}$) is 0.134 (0.213) Å longer than that of free nitrous oxide. The imaginary frequency of 97.8i $cm^{-1}$ for $TS_{D-G}$ is small in comparison with that of 363.2i $cm^{-1}$ for $TS_{C-F}$ although the N−N−O−Fe arrangement in $TS_{D-G}$ is quite similar to that of $TS_{C-F}$. The $C-O^1$ bond of 1.409 Å in G is slightly longer than that of free phenol 1.374 Å. Although the activation energy for $TS_{C-F}$ is 27.8 kcal/mol relative to C + nitrous oxide, its energy lies 2.5 kcal/mol below the dissociation limit of A + benzene. Therefore, no activation energy is required in principle to pass over $TS_{C-F}$ under adiabatic conditions. This oxygen insertion process is 20.0 kcal/mol exothermic, and the resultant intermediate F lies 50.3 kcal/mol below the dissociation limit. Thus, the decomposition of nitrous oxide on C is energetically preferred and can contribute to the preparation of the active iron−oxo species in a new catalytic cycle. On the other hand, if the decomposition of nitrous oxide occurs on intermediate D, this oxygen insertion is 58.2 kcal/mol exothermic (the energy difference of D and G). The occurrence of $TS_{D-G}$ should, therefore, be energetically more favorable than the release of phenol from intermediate D although it is clearly unfavorable in energy compared to the other pathway that begins with F, as shown in Figure 3. Thus, this reaction pathway can play a minor role in benzene hydroxylation over Fe−ZSM-5 zeolite. We will discuss later in the Appendix the reaction kinetics between these two pathways to gain a better understanding of this complicated catalytic reaction in the last section.

After the formation of F the reaction has another junction that leads to the two pathways indicated in Scheme 2. One reaction pathway via $TS_{F-G}$ leads to intermediate G that involves phenol and oxo ligands whereas the other one via $TS_{F-H}$ leads to intermediate H with hydroxo and phenoxo ligands. In the

**SCHEME 2**

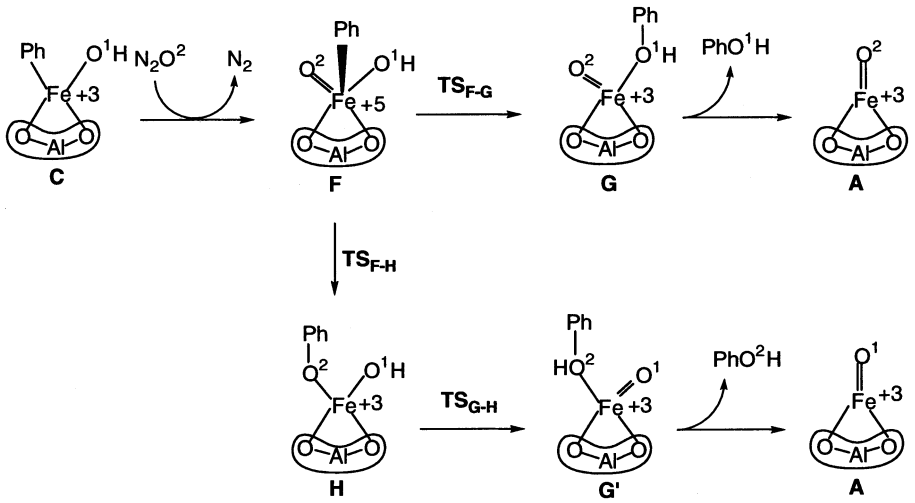


former pathway the initial complex A can be reproduced by the release of phenol from intermediate G whereas in the latter pathway intermediate H changes into G′ (=G) via $TS_{G-H}$ in which the formation of phenol occurs. The three intermediates F, G, and H can be connected via the transition states $TS_{F-G}$, $TS_{F-H}$, and $TS_{G-H}$. The transition states $TS_{F-G}$ and $TS_{F-H}$ correspond to phenyl shifts to the hydroxo and oxo ligands, respectively. $TS_{G-H}$ is a typical four-centered transition state for the H-atom migration from the hydroxo ligand to the phenoxo ligand, and the corresponding imaginary mode of vibration (1167i $cm^{-1}$) suggests that this transition state correctly connects H and G′.

Figure 3 also shows optimized geometries of the reaction species for these steps. Here let us look in detail at their geometries. Intermediates C and F have interesting Fe−C bonds of 1.968 and 1.999 Å, respectively. These Fe−C bonds are weak and easily broken; as a consequence, the relevant transition states, $TS_{C-D}$, $TS_{F-G}$, and $TS_{F-H}$, are early with respect to the cleavage of the corresponding Fe−C bond. Intermediate H involves hydroxo and phenoxo ligands with Fe−O distances of 1.766 and 1.788 Å, respectively. The transition vector of $TS_{F-G}$ ($TS_{F-H}$) with an imaginary frequency of 376i (304i) $cm^{-1}$ shows how the cleavage of the Fe−C bond and the formation of the C−O bond occurs. The Fe−C and C−O distances in $TS_{F-G}$ ($TS_{F-H}$) are 2.144 (2.091) and 1.962 (2.152) Å, respectively. The imaginary frequency of $TS_{G-H}$ 1167i $cm^{-1}$ is higher than that of $TS_{F-G}$ because $TS_{G-H}$ is responsible for the cleavage of a strong O−H bond whereas $TS_{F-G}$ is responsible for the phenyl shift. The $O^1$−H bond being broken and the $O^2$−H bond being formed in $TS_{G-H}$ were computed reasonably well to be 1.329 and 1.140 Å, respectively. DFT computations clearly demonstrate that the reaction pathway for the formation of H is energetically favorable in comparison with the direct convsersion (F → G) because $TS_{F-H}$ lies 6.9 kcal/mol below $TS_{F-G}$.

The two reaction pathways in Scheme 2 finally generate product phenol and reproduce the initial complex A. The release of phenol from G requires an activation energy of 23.8 kcal/mol whereas the total reaction for the conversion of benzene to phenol is 51.0 kcal/mol exothermic. Thus, this reaction is favorable in energy.

**Reaction Kinetics Analysis.** We summarize in Figure 4 the outline of our proposal for the catalytic cycle of benzene hydroxylation over Fe−ZSM-5 zeolite. Although this cycle looks complicated, it consists of benzene hydroxylation and oxygen insertion upon $N_2O$ decomposition. The benzene hydroxylation process begins with the interaction between benzene and A to lead to the benzene complex B; then, intermediate C is formed as a result of the benzene C−H bond activation on B. The recombination between the phenyl and hydroxo ligands leading to D can compete with the decomposition of nitrous oxide on C that leads to F. The two pathways finally reach the same complex G, and the release of phenol from G reproduces A, i.e., the initial complex in the catalytic cycle. Our DFT results demonstrate that the formation of intermediate F is more favorable in energy than that of intermediate D.

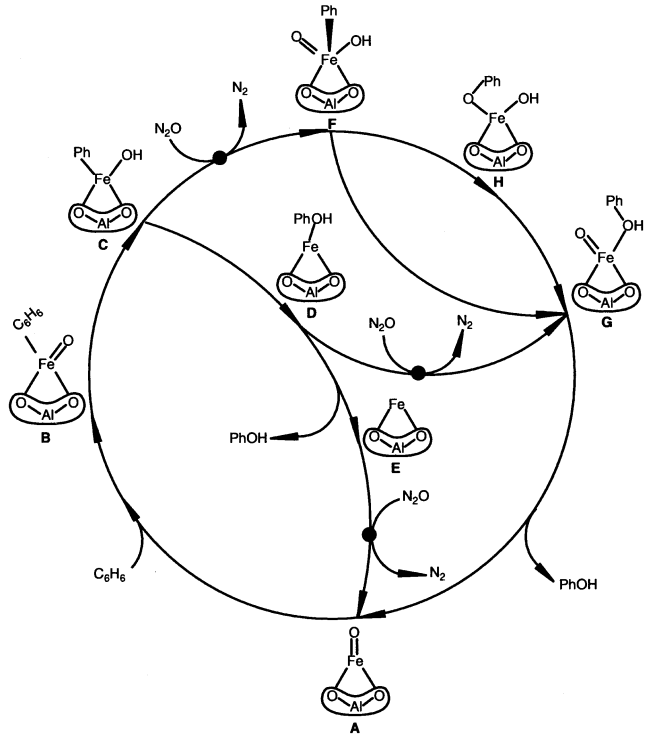


**Figure 4.** Possible catalytic cycle, in which the closed circles show oxygen insertion points upon decomposition of nitrous oxide.

We propose that in the catalytic reaction over Fe−ZSM-5 the benzene hydroxylation process and the decomposition of nitrous oxide should occur at the same active site in a well-balanced manner. If the balance of the two processes is lost, termination of the hydroxylation or overoxidation of phenol will occur. As discussed in the Appendix, quantity [F]/[D] is proportional to the square of the nitrous oxide concentration,

in which [D] and [F] are the concentrations of D and F, respectively. When the nitrous oxide concentration is zero, only intermediate D is, of course, produced under a single-turnover run. When the concentration of nitrous oxide is high, the reaction should proceed via intermediate F in the following way: C + $N_2O$ → $TS_{C-F}$ → F → $TS_{F-H}$ → H → $TS_{G-H}$ → G → A + $C_6H_5OH$. On the other hand, when the concentration of nitrous oxide is low, intermediate C is expected from reaction kinetics to lead to the decomposition of nitrous oxide immediately after the phenyl migration occurs. Thus, the reaction should proceed in the following way: C → $TS_{C-D}$ → D + $N_2O$ → $TS_{D-G}$ → G → A + $C_6H_5OH$.

## Summary and Conclusions

We have considered from B3LYP DFT computations how direct benzene hydroxylation occurs over Fe−ZSM-5 zeolite. We showed using a mononuclear iron model supported at the $AlO_4^-$ site of zeolite that the Fe−ZSM-5 system should reasonably catalyze the conversion of benzene to phenol with nitrous oxide. A key in this catalytic reaction is that benzene hydroxylation and $N_2O$ decomposition occur at the active site in a well-balanced manner. The total reaction is 51 kcal/mol exothermic per cycle. In the initial stages of the reaction, a reactive oxygen species called "α-oxygen" is formed upon decomposition of nitrous oxide at the iron active site. The first reaction step is the formation of the complex between benzene and the "α-oxygen" species. The C−H activation of benzene leads to an intermediate that involves OH and $C_6H_5$ groups as ligands. After forming this intermediate, the reaction branches into two possible pathways, depending on the concentration of nitrous oxide. According to a kinetics analysis, the recombination between the OH and $C_6H_5$ ligands, which leads to a complex of phenol, can occur when the concentration of nitrous oxide is low whereas the decomposition of nitrous oxide on the intermediate involving OH and $C_6H_5$ groups can occur when the nitrous oxide concentration is sufficiently high. We propose in this study that the hydroxylation reaction should proceed in the following way: (1) the formation of the benzene complex at the iron active site, (2) the hydrogen abstraction from benzene, (3) the decomposition of nitrous oxide at the active site, (4) the recombination between the OH and $C_6H_5$ ligands, and (5) the release of product phenol.

**Acknowledgment.** K.Y. acknowledges the Ministry of Education, Culture, Sports, Science, and Technology of Japan, Japan Society for the Promotion of Science, Japan Science and Technology Cooperation, and Takeda Science Foundation for their support of this work. A part of this work is supported by Kyushu University P & P "Green Chemistry". Computations were in part carried out at the Computer Center of the Institute for Molecular Science.

## Appendix

To refine the reaction mechanism, we investigated the reaction kinetics using the information about the potential energy diagrams obtained from DFT calculations. We assume that in the first step benzene is adsorbed at the "α-oxygen" site and the benzene C−H activation on B leads to C as in eq A1. Then,

$$A + C_6H_6 \xrightarrow{k_1} B \xrightarrow{k_2} C \qquad (A1)$$

there is a junction into the two reaction pathways: C → D → G and C → F → G. The energy difference between $TS_{C-D}$ and $TS_{C-F}$ is only 2.6 kcal/mol, so the two processes should be competitive. To gain a better understanding of this branching reaction, we evaluated the reaction mechanism using the following kinetic model:

$$C \xrightarrow{k_3} D + N_2O \xrightarrow{k_4} G \qquad (A2)$$

and

$$C + N_2O \xrightarrow{k_5} F \xrightarrow{k_6} G \qquad (A3)$$

Reactions A2 and A3 can be analytically solved to give the following solutions:

$$[D]_t = \frac{k_3 C_0}{k_4 n - (k_3 + k_5 n)}(e^{-(k_3 + k_5 n)t} - e^{-k_4 n t}) \qquad (A4)$$

and

$$[F]_t = \frac{k_5 n C_0}{k_6 - (k_3 + k_5 n)}(e^{-(k_3 + k_5 n)t} - e^{-k_6 t}) \qquad (A5)$$

where $C_0$ is the initial concentration of intermediate C, $n$ is the concentration of nitrous oxide, and $t$ is the time. DFT calculations predicted that the second step can easily occur in comparison with the first steps in both reactions A2 and A3. In reaction A2 the transition state for the phenyl migration lies 0.1 kcal/mol above the dissociation limit although that for the oxygen insertion step lies 20 kcal/mol below the dissociation limit. In reaction A3 the transition state for the oxygen insertion step lies 2.5 kcal/mol below the dissociation limit although that for the phenyl migration lies more than 35 kcal/mol below the dissociation limit. If we assume $k_3$, $k_5 n \ll k_4 n$, $k_6$, then the proportion of F to D is given by eq A6.

$$[F]/[D] = \frac{k_4 k_5}{k_3 k_6} n^2 \qquad (A6)$$

## References and Notes

(1) Iwamoto, M.; Hirata, J.; Matsukami, K.; Kagawa, S. *J. Phys. Chem.* **1983**, *87*, 903.

(2) (a) Panov, G. I.; Sobolev, V. I.; Kharitonov, A. S. *J. Mol. Catal.* **1990**, *61*, 85. (b) Panov, G. I.; Sheveleva, G. A.; Kharitonov, A. S.; Romannikov, V. N.; Vostrikova, L. A. *Appl. Catal. A: General* **1992**, *82*, 31. (c) Sobolev, V. I.; Kharitonov, A. S.; Paukshtis, Y. A.; Panov, G. I. *J. Mol. Catal.* **1993**, *84*, 117. (d) Sobolev, V. I.; Panov, G. I.; Kharitonov, A. S.; Romannikov, V. N.; Volodin, A. M.; Ione, K. G. *J. Catal.* **1993**, *139*, 435. (e) Panov, G. I.; Kharitonov, A. S.; Sobolev, V. I. *Appl. Catal. A: General* **1993**, *98*, 1. (f) Volodin, A. M.; Bolshov, V. A.; Panov, G. I. *J. Phys. Chem.* **1994**, *98*, 7548. (g) Dubkov, K. A.; Sobolev, V. I.; Talsi, E. P.; Rodkin, M. A.; Watkins, N. H.; Shteinman, A. A.; Panov, G. I. *J. Mol. Catal. A* **1997**, *123*, 155. (h) Panov, G. I.; Uriarte, A. K.; Rodkin, M. A.; Sobolev, V. I. *Catal. Today* **1998**, *41*, 365.

(3) (a) Suzuki, E.; Nakashiro, K.; Ono, Y. *Chem. Lett.* **1988**, 953. (b) Zholobenko, V. *Mendeleev Commun.* **1993**, 28. (c) Motz, J. L.; Heinichen, W. F. *J. Mol. Catal. A* **1998**, *136*, 175. (d) Häfele, M.; Roppelt, D.; Emig, G. *Appl. Catal. A* **1997**, *150*, 153. (e) Kucherov, A. V.; Shelef, M. *J. Catal.* **2000**, *195*, 106.

(4) See, for example: Morrison, R. T.; Boyd, R. N. *Organic Chemistry*, 6th ed.; Prentice Hall: New York, 1992; p 893.

(5) (a) Sobolev, V. I.; Dubkov, K. A.; Panna, O. V.; Panov, G. I. *Catal. Today* **1995**, *24*, 251. (b) Panov, G. I.; Sobolev, V. I.; Parmon, V. N.; Ovanesyan, N. S.; Shilov, A. E.; Shteinman, A. A. *React. Kinet. Catal. Lett.* **1997**, *61*, 251.

(6) Centi, G.; Cavani, F.; Trifirò, F. *Selective Oxidation by Heterogeneous Catalysis*; Kluwer Academic/Plenum Publishers: New York, 2001; p 346.

(7) (a) Trukhan, V. M.; Polukhov, V. V.; Sulimenkov, I. V.; Ovanesyan, N. S.; Dodonov, A. F. Shteinman, A. A. *Kinet. Catal.* **1998**, *39*, 788. (b) Ovanesyan, N. S.; Shteinman, A. A.; Dubkov, K. A.; Sobolev, V. I.; Panov, G. I. *Kinet. Catal.* **1998**, *39*, 792.

(8) Battiston, A. A.; Bitter, J. H.; Koningsberger, D. C. *Catal. Lett*. **2000**, *66*, 75.

(9) Chen. H.-Y.; Sachtler, W. M. H. *Catal. Today* **1998**, *42*, 73.

(10) Shilov. A. E.; Shteinman, A. A. *Acc. Chem. Res.* **1999**, *32*, 763.

(11) Reviews on sMMO: (a) Feig, A. L.; Lippard, S. J. *Chem. Rev.* **1994**, *94*, 759. (b) Lipscomb, J. D. *Annu. Rev. Microbiol.* **1994**, *48*, 371. (c) Liu, K. E.; Lippard, S. J. *Adv. Inorg. Chem.* **1995**, *42*, 263. (d) Wallar, B. J.; Lipscomb, J. D. *Chem. Rev.* **1996**, *96*, 2625. (e) Que, L., Jr.; Dong, Y. *Acc. Chem. Res.* **1996**, *29*, 190. (f) Valentine, A. M.; Lippard, S. J. *J. Chem. Soc., Dalton Trans.* **1997**, 3925. (g) Kurtz, D. M., Jr. *J. Biol. Inorg. Chem.* **1997**, *2*, 159. (h) Merkx, M.; Kopp, D. A.; Sazinsky, M. H.; Blazyk, J. L.; Müller, J.; Lippard, S. J. *Angew. Chem., Int. Ed. Engl.* **2001**, *40*, 2782.

(12) (a) Arbuznikov, A. V.; Zhidomirov, G. M. *Catal. Lett*. **1996**, *40*, 17. (b) Yakovlev, A. L.; Zhidomirov, G. M.; van Santen, R. A. *Catal. Lett.* **2001**, *75*, 45. (c) Yakovlev, A. L.; Zhidomirov, G. M.; van Santen, R. A. *J. Phys. Chem. B* **2001**, *105*, 12297.

(13) Joyner, R.; Stockenhuber, M. *J. Phys. Chem. B* **1999**, *103*, 5963.

(14) Feng, X.; Hall, W. K. *Catal. Lett.* **1997**, *46*, 11.

(15) Ryder, J. A.; Chakraborty. A. K.; Bell, A. T. *J. Phys. Chem. B* **2002**, *106*, 7059.

(16) (a) Yoshizawa, K.; Yumura, T.; Shiota, Y.; Yamabe, T. *Bull. Chem. Soc. Jpn*. **2000**, 73, 29. (b) Yoshizawa, K.; Shiota, Y.; Yumura, T.; Yamabe, T. *J. Phys. Chem. B* **2000**, *104*, 734.

(17) A review on the catalytic reactivities of the first-row transition-metal oxide ions ($MO^+$): Schröder, D.; Schwarz, H. *Angew. Chem., Int. Ed. Engl.* **1995**, *34*, 1973.

(18) (a) Schröder, D.; Schwarz, H. *Angew. Chem., Int. Ed. Engl*. **1990**, *29*, 1433. (b) Schröder, D.; Fiedler, A.; Hrusak, J.; Schwarz, H. *J. Am. Chem. Soc*. **1992**, *114*, 1215. (c) Schröder, D.; Schwarz, H.; Clemmer, D. E.; Chen, Y.-M.; Armentrout, P. B.; Baranov, V. I.; Böhme, D. K. *Int. J. Mass Spectrom. Ion Processes* **1997**, *161*, 175.

(19) (a) Schröder, D.; Schwarz, H. *Helv. Chim. Acta* **1992**, *75*, 1281. (b) Becker, H.; Schröder, D.; Zummack, W.; Schwarz, H. *J. Am. Chem. Soc.* **1994**, *116*, 1096. (c) Ryan, M. F.; Stöckigt, D.; Schwarz, H. *J. Am. Chem. Soc.* **1994**, *116*, 9565.

(20) (a) Yoshizawa, K.; Shiota, Y.; Yamabe, T. *Chem. Eur. J*. **1997**, *3*, 1160. (b) Yoshizawa, K.; Shiota, Y.; Yamabe, T. *J. Am. Chem. Soc.* **1998**, *120*, 564. (c) Yoshizawa, K.; Shiota, Y.; Yamabe, T. *Organometallics* **1998**, *17*, 2825. (d) Yoshizawa, K.; Shiota, Y.; Yamabe, T. *J. Chem. Phys.* **1999**, *111*, 538. (e) Yoshizawa, K.; Shiota, Y.; Kagawa, Y.; Yamabe, T. *J. Phys. Chem. A* **2000**, *104*, 2552. (f) Shiota, Y.; Yoshizawa, K. *J. Am. Chem. Soc.* **2000**, *122*, 12317. (g) Shiota, Y.; Yoshizawa, K. *J. Chem. Phys.* **2003**, *118*, 5872.

(21) Yoshizawa, K.; Shiota, Y.; Yamabe, T. *J. Am. Chem. Soc.* **1999**, *121*, 147.

(22) (a) Yoshizawa, K.; Kagawa, Y. *J. Phys. Chem. A* **2000**, *104*, 9347. (b) Yumura, T.; Yoshizawa, K. *Organometallics* **2001**, *20*, 1397. (c) Yumura, T.; Amenomori, T.; Kagawa, Y.; Yoshizawa, K. *J. Phys. Chem. A* **2002**, *106*, 621.

(23) (a) Becke, A. D. *Phys. Rev. A* **1988**, *38*, 3098. (b) Becke, A. D. *J. Chem. Phys.* **1993**, *98*, 5648.

(24) Lee, C.; Yang, W.; Parr, R. G. *Phys. Rev. B* **1988**, *37*, 785.

(25) Baker, J.; Muir, M.; Andzelm, J.; Scheiner, A. In *Chemical Applications of Density-Functional Theory*; Laird, B. B., Ross, R. B., Ziegler, T., Eds.; ACS Symposium Series 629; American Chemical Society: Washington, DC, 1996.

(26) Wachters, A. J. H. *J. Chem. Phys.* **1970**, *52*, 1033.

(27) Hay, P. J. *J. Chem. Phys.* **1977**, *66*, 4377.

(28) Raghavachari, K.; Trucks, G. W. *J. Chem. Phys*. **1989**, *91*, 1062.

(29) Dunning, T. H.; Hay, P. J. In *Modern Theoretical Chemistry*; Schaefer, H. F., III, Ed.; Plenum: New York, 1976; Vol. 3, p 1.

(30) Frisch, M. J.; Trucks, G. W.; Schlegel, H. B.; Scuseria, G. E.; Robb, M. A.; Cheeseman, J. R.; Zakrzewski, V. G.; Montgomery, J. A.; Stratmann, R. E.; Burant, J. C.; Dapprich, S.; Millam, J. M.; Daniels, A. D.; Kudin, K. N.; Strain, M. C.; Farkas, O.; Tomasi, J.; Barone, V.; Cossi, M.; Cammi, R.; Mennucci, B.; Pomelli, C.; Adamo, C.; Clifford, S.; Ochterski, J.; Petersson, G. A.; Ayala, P. Y.; Cui, Q.; Morokuma, K.; Malick, D. K.; Rabuck, A. D.; Raghavachari, K.; Foresman, J. B.; Cioslowski, J.; Ortiz, J. V.; Baboul, A. G.; Stefanov, B. B.; Liu, G.; Liashenko, A.; Piskorz, P.; Komaromi, I.; Gomperts, R.; Martin, R. L.; Fox, D. J.; Keith, T.; Al-Laham, M. A.; Peng, C. Y.; Nanayakkara, A.; Gonzalez, C.; Challacombe, M.; Gill, P. M. W.; Johnson, B. G.; Chen, W.; Wong, M. W.; Andres, J. L.; Head-Gordon, M.; Replogle, E. S.; Pople, J. A. *Gaussian 98*; Gaussian Inc.: Pittsburgh, PA, 1998.